Journal of Inorganic and Organometallic Polymers and Materials (2020) 30:1609–1620
https://doi.org/10.1007/s10904-019-01308-8

Novel 1,3,4-Thiadiazolethiosemicarbazones Derivatives and Their Divalent Cobalt-Complexes: Synthesis, Characterization and Their Efficiencies for Acidic Corrosion Inhibition of Carbon Steel

Tahani M. Bawazeer[1,2] · Hoda A. El-Ghamry[1,3] · Thoraya A. Farghaly[4] · Ahmed Fawzy[1,5]

Received: 28 June 2019 / Accepted: 29 August 2019 / Published online: 5 September 2019

Abstract

Two newly synthesized ligands based on 1,3,4-thiadiazolethiosemicarbazone have been isolated by the condensation reaction of 2,3-disubstituted-5-acetyl-1,3,4-thiadiazole derivatives with thiosemicarbazide in acidic medium in addition to their Co(II) chelates. The synthesized cobalt chelates that have been obtained by the reaction of each ligand with cobalt acetate were confirmed to have the formulae [(**LM**)Co(OAc)$(H_2O)_2$]H_2O (**LM–Co**) and [(**LN**)Co(OAc)$(H_2O)_2$]0.5CH_3OH (**LN–Co**); where **LM** and **LN** are 1,3,4-thiadiazolethiosemicarbazone ligands with methyl and nitro substituents, respectively. Comparison of the IR spectrum of each ligand with that of its cobalt complex implied that both ligands acted as monobasic tridentate connecting to the cobalt ion through N atoms of both azomethine group and thiadiazole ring and S atom of deprotonated SH group as well. The two complexes have been proved to have octahedral geometrical structures. The synthesized compounds were studied as corrosion inhibitors for carbon steel in molar hydrochloric acid solution using several chemical and electrochemical techniques. The investigational outcomes displayed that the inhibition efficiencies of the examined compounds were found to augment as the concentrations of such compounds raised. At comparable inhibitors concentration, the inhibition efficiency was a little increased following the order: **LM > LM–Co > LN > LN–Co**. The acquired high inhibition efficiencies of the explored compounds were ascribed to the potent adsorption of the molecules on the steel surface and construction of adherent layers. Such adsorption was found to accord with Langmuir adsorption isotherm. There is a good correlation in the results obtained from the different measurements used.

Keywords Thiadiazoles · Thiosemicarbazone · Cobalt chelates · Acidic corrosion · Inhibition

1 Introduction

Heterocyclic ligands with more than one hetero-atom as sulfur and nitrogen are versatile multi-donor in coordination chemistry [1–3], among them, polyfunctional electron rich-1,3,4-thiadiazoles. In the last two decades, ligands carrying thiadiazole moiety revealed a considerable number of publications concerned with the preparation, structural elucidation and implementations of metal complexes of this type of ligands [4–7]. As for instance, copper and nickel complexes based on 1,3,4-thidiazole ligands display potent antimicrobial activity and were found to be able to protect tomato against Verticillium wilt [8, 9].

It was stated [10–12] that thiadiazole ring itself was used for steel corrosion protection and showed a high efficiency in different acidic media, while, the application of their complexes in the area of corrosion inhibition is limited [2]. Researchers are paying much attention to the search for

✉ Hoda A. El-Ghamry
helghamrymo@yahoo.com

1 Chemistry Department, Faculty of Applied Science, Umm Al-Qura University, Makkah, Saudi Arabia

2 Medical Applications of Nanobiotechnology Research Group, King Fahad Medical Research Center, King Abdulaziz University, Jeddah, Saudi Arabia

3 Chemistry Department, Faculty of Science, Tanta University, Tanta, Egypt

4 Chemistry Department, Faculty of Science, Cairo University, Giza, Egypt

5 Chemistry Department, Faculty of Science, Assiut University, Assiut, Egypt

compounds that act as corrosion inhibitors because of their serious problems with metals and their alloys [13–17]. The metal corrosions cause many industrial problems including the deterioration of buildings and machinery, the erosion of boilers in factories and oil pipelines in oil refineries and others, which leads to shortening the life of these facilities and low operational efficiencies of them [18]. Also, thiosemicarbazone derivatives having nitrogen and sulfur atoms play a vital role as corrosion inhibitors [19, 20]. Recently, Quraishi et al. [21] published an irreplaceable review article where it displayed the substituent effect of the organic compounds on the efficiency of the corrosion inhibitors. They stated that the inhibition effectiveness was promoted in the presence of electron donating substituents while corrosion inhibition potential was reduced with existence of electron withdrawing substituents [22, 23]. Exceptions to this popularization have been noted in few reported articles though [24]. Based on these knowledge, we designed two new corrosion inhibitors depending on 1,3,4-thiadiazolethiosemicarbazone compound with one electron donating substituent (i.e. CH_3) and one electron withdrawing substituent (i.e. NO_2) as well as their Co(II) complexes. Our objective behind such synthesis and structure characterization of the designed compounds is to investigate their corrosion inhibition efficiency of steel in acid medium which expected to increase due to the presence of many sulfur and nitrogen atoms as well as the existence of cobalt metal in addition to examination of the effect of electron donating and electron withdrawing substituents on their corrosion inhibition efficiency.

2 Experimental

2.1 Materials and Methods

All used reagents in this study were of very pure and obtained from BDH, Aldrich or Sigma. The utilized solvents for recording all spectral investigations in this text were bought with high purity from Aldrich. The elemental microanalyses [C, H, N] of the synthesized derivatives were carried out at Cairo University, in the microanalytical center on Perkin-Elmer 2400 CHN Elemental analyzer. The Infrared (IR) spectra were performed on a 1430-Perkin-Elmer infrared-spectrophotometer ranging from 4000 to 200 cm^{-1} as sample-KBr discs. The NMR spectra were carried out in dimethyl sulfoxide (DMSO-d_6) or chloroform ($CDCl_3$) on ^{1}H-NMR (Varian operating at 400 MHz) and ^{13}CNMR (Varian operating at 100 MHz). A Finnigan-MAT8222 spectrometer was utilized for recording the electron impact mass spectra for all samples at 70 eV at Cairo University, in Micro-analytical center. The solid complexes magnetic susceptibility was recorded at ordinary temperature by using magnetic susceptibility instrument via the Gouy's technique. Thermogravimetric analysis (TGA) of the two prepared solid complexes were recorded on the TG-50-Schimadzu thermogravimetric analyzer under 10 °C/min heating rate/nitrogen atmosphere with temperature ranging from 25 to 800 °C. Corrosion inhibition investigations were conveyed out on carbon steel rods (the working electrode having the composition, wt%: %C = 0.11, %Si = 0.25, %S = 0.05, %P = 0.04, %Mn = 0.45 and the remainder is iron). Experiments of weight-loss (WL), as a chemical technique, were performed in a temperature-controlled system. Carbon steel samples were cylindrical rods of areas closed to 12 cm^2 and were prepared for such measurements as stated previously [16, 17]. Electrochemical measurements (potentiodynamic polarization (PP) and electrochemical impedance spectroscopy (EIS)) were conducted using PGSTAT30 potentiostat/galvanostat. The working electrode was in the form of a carbon steel rod compressed into a Teflon holder in which the exposed electrode area to the corrosive media was 0.5 cm^2. Before each experiment the working electrode was treated as in WL measurements, then it was inserted immediately into a 100 ml of the corrosive medium (1.0 M HCl, blank) and/or the perquisite inhibitor concentration at open circuit potential (OCP) for about 60 min or until a steady state was attained. In a PP technique, the electrode potential was altered automatically from − 200 to + 200 mV versus OCP whereas EIS runs were conveyed out at a frequency range of 100 kHz to 0.1 Hz with amplitude of 4.0 mV peak-to-peak using AC signals at OCP.

2.2 Synthesis of Organic Ligands (LM and LN)

The two thiadiazole thiosemicarbazone ligands **LM** and **LN** have been prepared as described in Scheme 1 from the condensation reaction of 0.01 mol of 5-acetyl-3-aryl-2-imino-1,3,4-thiadiazole-derivatives (**1** or **3**) [25] and 0.01 mol of thiosemicarbazide with addition of 1 mL of conc. HCl in 30 mL EtOH under ordinary reflux for 5 h. The solid products, which resulting out after cooling, have been filtered under vacuum and recrystallized from mixture of ethanol and dioxane to give the two ligands **LM** and **LN**.

2.3 Preparation Cobalt Complexes (LM–Co and LN–Co)

Addition of hot solution of 0.001 mol of cobalt acetate tetrahydrate (0.249 g of $Co(CH_3COO)_2{\cdot}4H_2O$), dissolved in hot methanol, portion wise to hot 20 mL methanolic solution containing 0.001 mol of each of ligands **LM** or **LN** (0.306 g or 0.337 g, respectively). The clear mixture has been refluxed for 2 h at 65 °C within which colored products were appeared. The formed solid of thiadiazole–cobalt complexes **LM–Co** and **LN–Co** were filtered under vacuum

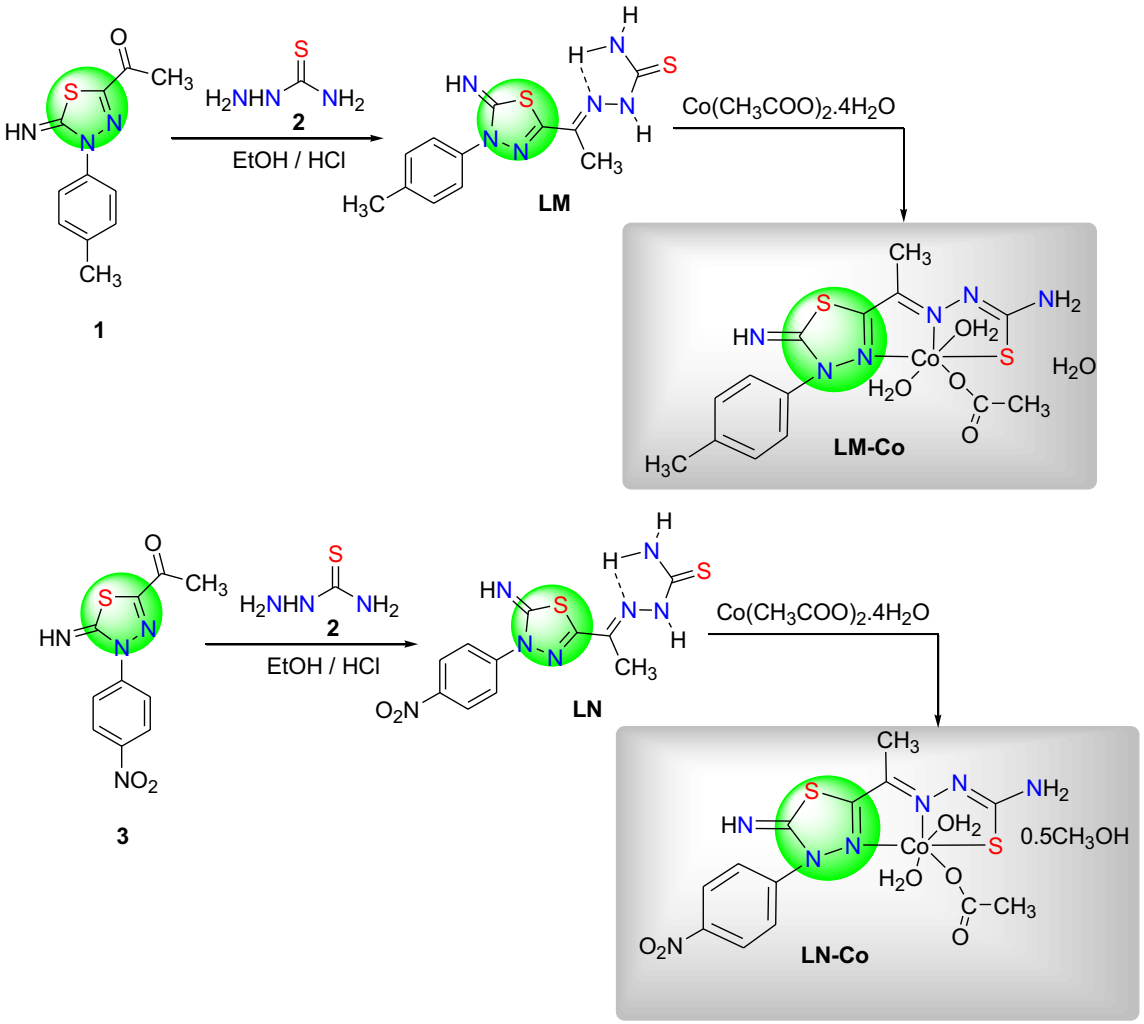

Scheme 1 Synthetic routs and structures of the organic ligands and their Co(II) complexes

from the hot solutions, and then methanol and ether were used to wash the precipitate that finally dried under vacuum.

3 Results and Discussion

Information about the molecular formulae of the synthesized ligands and their metal complexes along with their empirical formulae, molecular weights, colors, melting points, molar conductance and analytical results are depicted in Table 1. Analysis of the obtained organic ligands (**LM** and **LN**) and their Co(II) complexes (**LM–Co** and **LN–Co**) using elemental analysis tool indicated that the structures of the synthesized compounds are matching well with the prophesied molecular formulae depicted in Table 1. These results assisted forming of the Co(II) chelates in 1:1 (M:L) molar ratio. Recording of the molar conductance from 10^{-3} M solution of the compounds **LM–Co** and **LN–Co** in DMF indicated the non-electrolytic nature of the two compounds ($\Lambda = 19.4$ and 21.2 Ω^{-1} cm^2 mol^{-1} for **LM–Co** and **LN–Co**, respectively) [26, 27].

The compounds also were noticed to be highly air and moisture stable. They dissolved easily in almost all highly polar organic solvent but hardly soluble in non-polar ones.

3.1 ^{1}H and ^{13}C NMR Spectra of the Organic Ligands LM and LN

The structures of the two thiadiazole ligands, **LM** and **LN**, were assured from their ^{1}H NMR and ^{13}C NMR spectra. In detail, ^{1}H NMR of p-CH_3 substituted thiadiazole ligand **(LM)** showed six singlet signals and in addition to two doublet signals at $\delta = 1.59$ (s, CH_3), 2.34 (s, CH_3), 6.40, (s, NH), 7.10 (d, Ar–H), 7.30 (s, NH), 7.31(d, Ar–H), 8.33 (s, NH), 8.80 (s, NH) (Fig. 1). On the other hand, ^{1}H NMR of p-NO_2 substituted thiadiazole ligand (**LN**) revealed

Table 1 Micro-analysis and physical properties of the synthesized ligands and their cobalt complexes

Comp. no.	Molecular formula (empirical formulae)	Color (mol. wt.)	$(\Lambda_m)^a$	M.p. (yield)	Microanalysis, calc. (found) (%)			
					C	H	N	M[c]
LM	$C_{12}H_{14}N_6S_2$	Orange (306.41)	–	218[b] (86%)	47.04 (47.11)	4.61 (4.53)	27.43 (27.55)	–
LM–Co	$[(LM)Co(OAc)(H_2O)_2]H_2O$ $C_{14}H_{22}N_6O_5S_2Co$	Reddish brown (477.42)	19.4	> 300 (69%)	35.22 (35.13)	4.64 (4.51)	17.60 (17.74)	12.34 (12.11)
LN	$C_{11}H_{11}N_7O_2S_2$	Gold (337.38)	–	102 (91%)	39.16 (39.24)	3.29 (3.15)	29.06 (29.13)	–
LN–Co	$[(LN)Co(OAc)(H_2O)_2]0.5CH_3OH$ $C_{13.5}H_{19}N_7O_{6.5}S_2Co$	Deep brown (506.4)	21.2	> 300 (76%)	32.02 (32.28)	3.78 (3.62)	19.36 (19.39)	11.64 (11.51)

[a]Molar conductivity (Ω^{-1} cm^2 mol^{-1}) of 10^{-3} M solution in DMF

[b]Decomposition temperature

[c]Calculated from TG thermograms

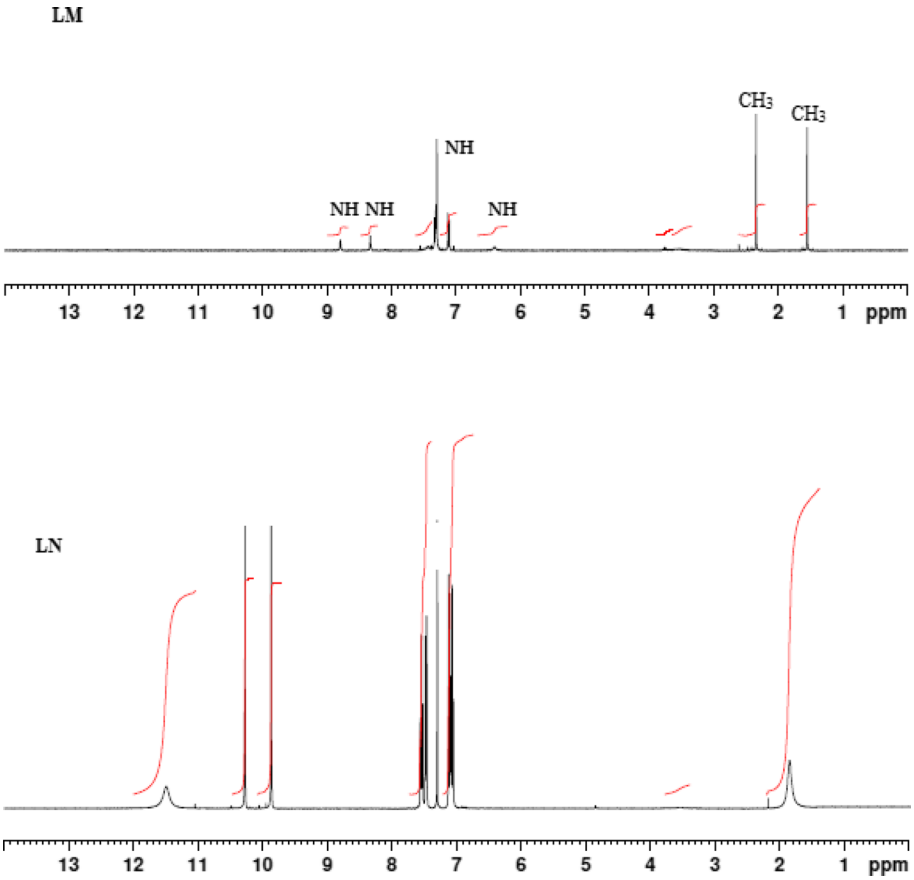

Fig. 1 1H-NMR spectra of the two ligands **LM** and **LN**

the characteristic signals for the suggested structure as follows: one singlet signals for methyl group at δ = 1.8; four NH singlet signals at δ = 7.3, 9.9, 10.3 and 11.5; in addition to two doublet with two proton intigration for four aromatic protons at δ = 7.10 and 7.46 ppm (Fig. 1). It is important to noted that the disappearance of NH_2 at δ = 4–6 ppm in ^{1}H NMR of the two ligands **LM** and **LN** can be attributed to the existance of H-bond between one proton of NH_2 and N=C groups which leads to the non-equivalent two protons of the amino group of thiosemicarbazone moiety [28] as presented in Scheme 1. Also, all the remarkable carbon signals for the two thiadiazole ligands **LM** and **LN** are in agreement with the suggested structure as follows: **LM** ligand: ^{13}C NMR δ 14.0 (CH_3), 18.6 (CH_3), 127.2, 127.4, 129.8, 133.8, 140.9, 142.6, 145.7,

179.2 (C=S). **LN** ligand: ^{13}C NMR δ 15.19 (CH_3), 115.5, 117.9, 120.3, 1323.9, 135.5, 160.1, 164.8, 179.0 (C=S).

3.2 FT-IR Spectra

Determination of the coordination sites in the organic ligand that take part in coordination to metal ion can easily be identified by careful comparison of FT-IR spectrum of each ligand with that of its metal complex. Function groups which participate in bond formation, usually, subjected to a shift in band positions and/or intensities while some other peaks completely disappear after complexation. The most significant IR bands shown by the organic ligands and their Co(II) complexes are indicated in Table 2.

The two compounds **LM** and **LN** showed two bands at 3410 and 3227 cm^{-1} in the spectrum of **LM** and at 3454 and 3250 cm^{-1} in the spectrum of **LN** corresponding to $\nu(NH_2)$ asy and $\nu(NH_2)$sym. The band appearing in the spectra of **LM** and **LN** ligands at 3141 and 3183 cm^{-1} assigned to ν(NH) of the imino group [29]. Such vibrations appeared, in the spectra of cobalt chelates, nearly at the same values confirming that these groups remained free in the metal chelates. Some bands underwent shift in their position to higher or lower wavenumbers in spectra of metal complexes due to H-bond formation [30].

The spectra of **LM** and **LN** did not show any bands within 2500–2700 cm^{-1} region which thioimide group usually appears (ν(SH)). This supports that the two ligands exist in the thione form in the solid state which cancel the probability of thioamide-thioimidol tautomerism (H–N–C=S, N=C–SH) [31].

The three bands that appeared in the spectrum of **LM** at 1596, 1297 and 792 cm^{-1} and in the spectrum of **LN** at 1617, 1256 and 769 cm^{-1} were assigned to ν(C=N), ν(C=S) and δ(C=S) bands, respectively. These bands underwent a shift in their position appearing in the spectrum of **LM–Co** at 1603, 1317 and 782 cm^{-1} and in the spectrum of **LN–Co** at 1601, 1265 and 762 cm^{-1} indicating the coordination of the azomethine nitrogen and thiolate sulfur to the metal center [31]. The involvement of the azomethine nitrogen in coordination to Co atom is further supported by the shift in position of ν(N–N) band that appeared in the spectrum of **LM** and **LN** at 1032 and 1144 cm^{-1} and also by the appearance of new bands in the spectra of **LM–Co** and **LN–Co** at 437 and 453 cm^{-1}, respectively, which assignable to ν(M–N).

The new bands which appeared in the spectrum of **LM–Co** at 1556 and 1344 cm^{-1}, and in the spectrum of **LN–Co** at 1545 and 1328 cm^{-1} assigned to $\nu_{asy}(CH_3COO)$ and $\nu_{sym}(CH_3COO)$ group, successively. The difference between each two bands was found to be 212 and 217 cm^{-1} for **LM–Co** and **LN–Co**, respectively, meaning the coordination mode of the carboxylate group in these complexes is monodentate mode [32, 33].

3.3 Thermogravimetric Analysis

Thermogravimetric analysis is one of the most useful methods which used to extensively study the thermal behavior of inorganic compounds and illustrate to what extent the metal chelates are thermally stable. It is also being applied to conclude the coordination behavior of the metal chelates by affording knowledge exemplary information about their thermal steps, intermediates as well as residues that are left behind after complete decomposition of the compounds [34]. Moreover, the percent of lattice or coordinated water and solvent molecules in addition to anion groups can be precisely calculated and determined from TG thermograms. Accordingly, the two cobalt chelates, **LM–Co** and **LN–Co**, were subjected to TG/DTG measurements. Detailed thermo-analytical results for the two complexes **LM–Co** and **LN–Co** are depicted in Table 3 and represented in Fig. 2.

Accurate analysis of the Co chelates, **LM–Co** and **LN–Co**, thermograms revealed that the two compounds underwent degradation in five and four successive steps, respectively, in the range 28-800 °C.

LM–Co complex underwent degradation as shown behind:

$$H_2O \xrightarrow[[-3.59(calcd.3.77\%)]]{32-81\,^{\circ}C} [(LM)Co(OAc)(H_2O)_2]$$

$$[(LM)Co(OAc)(H_2O)_2] \xrightarrow[[-7.59(calcd.7.54\%)]]{81-177\,^{\circ}C} [(LM)Co(OAc)]$$

$$[(LM)Co(OAc)] \xrightarrow[[-15.95(calcd.15.50\%)]]{177-300\,^{\circ}C} [(LM)Co]$$

$$[(LM)Co] \xrightarrow[[-49.47(calcd.48.86\%)]]{300-592\,^{\circ}C} Intermediate\,1$$

$$Intermediate\,1 \xrightarrow[[-4.60(calcd.5.44\%)]]{592-800\,^{\circ}C} CoS$$

Table 2 Assignments for diagnostic important bands in IR spectra of the synthesized ligands and their cobalt complexes

Compound	νNH_2, νNH	νC–H sp^3	νC=N	νN–N	δNH	νC=S	νM–N
LM	3410, 3227, 3141	2965	1596	1032	1494	1297, 792	
LM–Co	3426, 3291, 3187	2927	1603	1016	1488	1317, 782	437
LN	3454, 3250, 3180	2978	1617	1144	1482	1256, 769	–
LN–Co	3426, 3217, 3190	2984	1601	1137	1480	1265, 762	453

Table 3 The decomposition stages, temperature ranges, computed and experimental weight lacks of complexes **LM–Co** and **LN–Co**

Complex no. (mol. wt.)	Temp. range (°C)	Mass loss %		Assignment
		Calc.	Exp.	
LM–Co	32–81	3.77	3.59	Loss of one lattice H_2O molecule
$[(LM)Co(OAc)(H_2O)_2]\cdot H_2O$	81–177	7.54	7.49	Loss of two coordinated H_2O
(477.42)	177–300	15.50	15.95	Loss of one coordinated $CH_3COO^- + CH_3$ group
	300–592	48.86	49.47	Loss of $C_{10}H_9N_5S$ moiety
	592–800	5.44	4.60	Further decomposition of ligand leaving CoS
		12.34	12.11	% of metal content.
LN–Co	25–60	3.15	3.8	Loss of half lattice CH_3OH molecule
$[(LN)Co(OAc)(H_2O)_2]0.5CH_3OH$	60–204	24.11	24.24	Loss of two coordinated H_2O_+ one coordinated CH_3COO^- group
(506.4)	204–355	12.05	12.19	Loss of one $CH_3 + NO_2$ groups
	355–800	11.47	10.89	Further decomposition of ligand leaving CoS + 13C.
		11.64	11.51	% of metal content.

Whereas LN-Co chelate was decomposed as shown below:

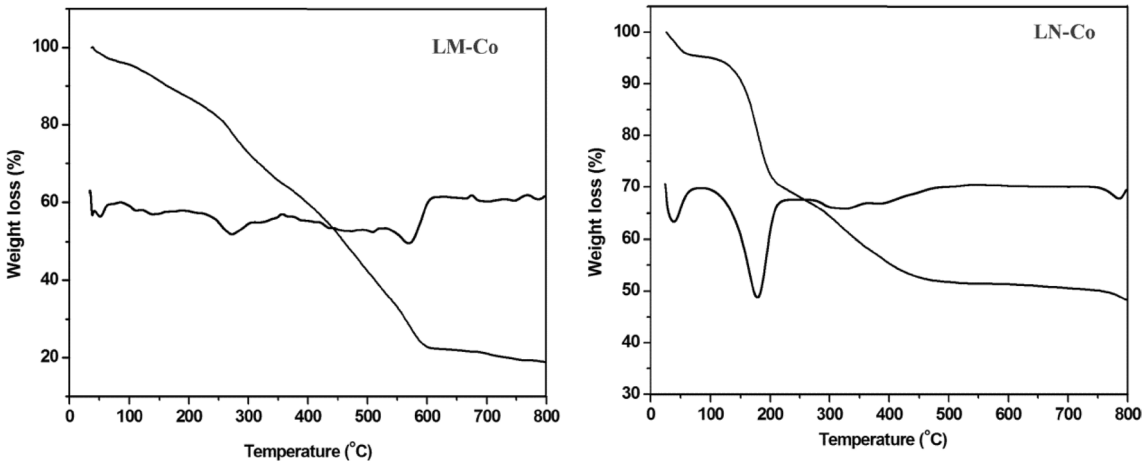

Fig. 2 TG/DTG thermograms of the two Co(II) chelates **LM–Co** and **LN–Co**

$$0.5CH_3OH \xrightarrow[[-3.8(calcd.3.15\%)]]{25-60\,^{\circ}C} [(LM)Co(OAc)(H_2O)_2]$$

$$[(LM)Co(OAc)(H_2O)_2] \xrightarrow[[-24.24(calcd.24.11\%)]]{60-204\,^{\circ}C} [(LM)Co]$$

$$[(LM)Co] \xrightarrow[[-12.19(calcd.12.05\%)]]{204-355\,^{\circ}C} \text{Intermediate 1}$$

$$\text{Intermediate 1} \xrightarrow[[-10.89(calcd.11.47\%)]]{355-800\,^{\circ}C} CoS + \text{carbonresidue}$$

.

3.4 UV–Vis Spectra and Magnetic Moment Measurements

Electronic spectral tool is one of the main methods of analysis that is used to assign the type of geometrical structure exhibited by the metal center in metal complexes. It is also very useful to assign the type of electronic transitions exhibited by different functions groups in both organic and inorganic compounds.

The UV–Vis spectra of the two ligands **LM** and **LN** and their Co(II) chelates were recorded as solid samples using Nujol mull technique. For the free ligands, **LM** and **LN**, their spectra exhibited two bands at 250 and 284 nm for **LM** and at 244 and 289 cm^{-1} for **LN** that assigned to assigned to $\pi \rightarrow \pi^*$ transitions of aromatic benzene ring and azomethine groups, respectively. The band that appeared at 336

and 355 nm in the spectra of **LM** and **LN**, respectively, assigned to n → π* transition of azomethine groups. In the spectra of cobalt complexes, **LM–Co** and **LN–Co**, such bands have shifted to longer wavelengths (appeared at 252, 303 and 347 nm in the spectrum of **LM–Co** and at 258, 299 and 367 nm in the spectrum of **LN–Co**) as a consequence of coordination of the azomethine nitrogen to the metal center [35, 36].

The electronic spectra of **LM–Co** and **LN–Co** complex exhibited two bands at 515 and 678 cm^{-1} in the spectrum of **LM–Co** and at 540 and 676 cm^{-1} in the spectrum of **LN–Co** assignable to $^4T_{1g}(F) \rightarrow {}^4T_{1g}(p)$ and $^4T_{1g}(F) \rightarrow {}^4A_{2g}(F)$ transitions, respectively, supporting octahedral configuration [37, 38]. Such complexes exhibited μ_{eff} of 4.55 and 4.61 B.M for **LM–Co** and **LN–Co** which are characteristic of high-spin octahedral complexes. Based on the previous results the structures of **LM–Co** and **LN–Co** complexes can be illustrated as shown in Scheme 1.

3.5 Estimation of the Inhibition Efficiencies of the Synthesized Compounds

3.5.1 Weight-Loss Measurements

Weight-loss measurements of carbon steel in 1.0 M HCl were conveyed out in the absence and presence of several concentrations of the synthesized compounds (**LM**, **LN**, **LM–Co**, **LN–Co**) in the concentration range (100–900 ppm) at 25 °C. Similar weight loss curves illustrated in Fig. 3 obtained for the ligand **LM** were acquired for other compounds did not appear here. Values of the corrosion rates (CR) in mils penetration per year (mpy) of carbon steel (listed in Table 4) were computed from the following equation [39]:

$$\mathrm{CR\,(mpy)} = \frac{KW}{Atd}, \tag{1}$$

where K is a constant equals 3.45×10^6, W is the weight-loss (g), A is area of the steel sample (cm^2), t is time (h) and d is the density of carbon steel (7.86 g/cm^3). The values of the inhibition efficiencies (% IE) and the degree of surface coverage (θ) of the synthesized compounds for the corrosion of carbon steel (Table 4) were determined as follows [40]:

$$\%\mathrm{IE} = \theta \times 100 = \left[1 - \frac{CR_{inh}}{CR}\right] \times 100 \tag{2}$$

where CR and CR_{inh} are corrosion rates in the absence and containing the inhibitor, respectively.

The acquired outcomes showed that CR value was found to decrease with the inhibitors concentrations as a result of augmented adsorption coverage of the inhibitors on the surface of carbon steel with the inhibitor concentration causing a decrease in the dissolution rates of steel alloy. Therefore, the synthesized compounds can be regarded as effective inhibitors for carbon steel corrosion in the investigated

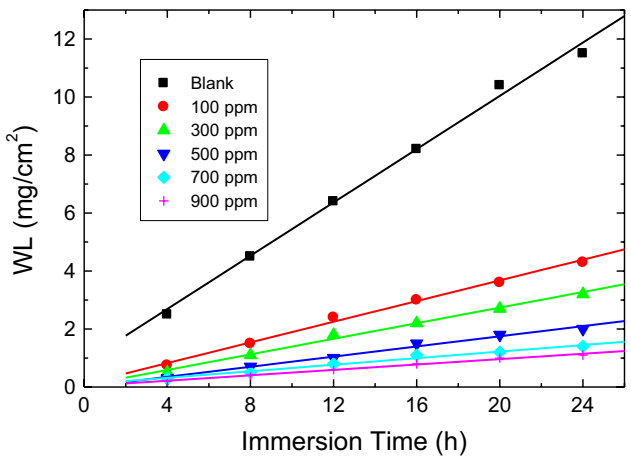

Fig. 3 Weight-loss versus immersion time of carbon steel corrosion in 1.0 M HCl solution in the absence and presence of different concentrations of the ligand **LM** at 25 °C

Table 4 Values of **CR** (in mpy) of carbon steel, **% IE** and **θ** of several concentrations of the synthesized compounds in 1.0 M HCl solution at 25 °C

Inh.	Concn. (ppm)	CR (mpy)	% IE	θ
	0	**241**	–	–
LM	100	77	68	0.68
	200	51	79	0.79
	300	34	86	0.86
	400	22	91	0.91
	500	17	93	0.93
LN	100	89	63	0.63
	200	58	76	0.76
	300	38	84	0.84
	400	27	89	0.89
	500	24	90	0.90
LM–Co	100	82	66	0.66
	200	58	76	0.76
	300	38	84	0.84
	400	27	89	0.89
	500	22	91	0.91
LN–Co	100	94	61	0.61
	200	68	72	0.72
	300	46	81	0.81
	400	36	85	0.85
	500	28	88	0.88

Bold font is given to discriminate the compounds codes

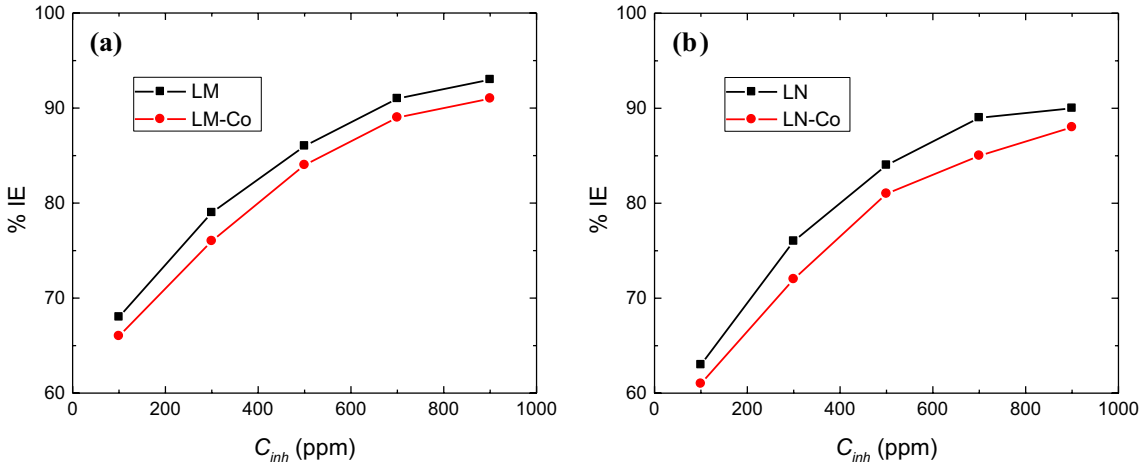

Fig. 4 Variation of inhibition efficiencies with the concentrations of the synthesized ligands and their complexes: **a LM**, **b LN**, for the corrosion of carbon steel in 1.0 M HCl solution at 25 °C

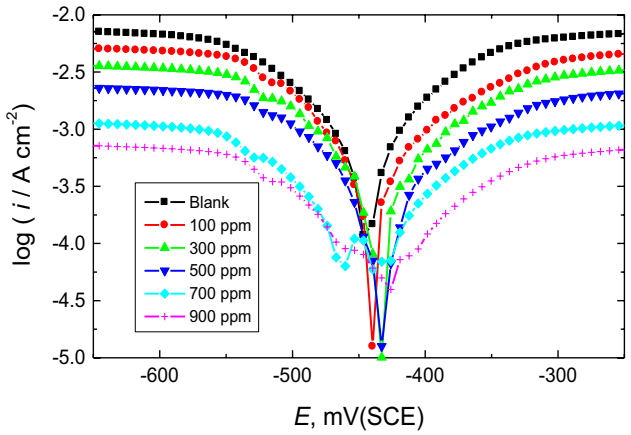

Fig. 5 Potentiodynamic polarization curves of carbon steel corrosion in 1.0 M HCl solution in the absence and presence of different concentrations of the ligand **LN** at 25 °C

aggressive medium (1.0 M HCl). At comparable inhibitors concentrations, the inhibition efficiencies (illustrated in Fig. 4) were found to be slightly increased in the order: **LM > LM–Co > LN > LN–Co** designating that the possible steric impacts and electronic density of donor atoms of the examined compounds are considered as the principle roles in the adsorption process.

3.5.2 Potentiodynamic Polarization (PP) Measurements

The PP measurements for carbon steel in 1.0 M HCl in the absence and presence of several concentrations of the synthesized compounds are carried out at 25 °C. Only PP curves obtained for the ligand **LN** as an example is presented here in Fig. 5 and the related corrosion parameters are assessed and are inserted in Table 5. The values of % IE and θ of the synthesized compounds were calculated from the equation:

$$\%\,\mathrm{IE} = \theta \times 100 = \left[1 - \frac{i_{corr(inh)}}{i_{corr}}\right] \times 100 \tag{3}$$

where, i_{corr} and $i_{corr(inh)}$ are corrosion current densities in the absence and presence of the inhibitor, respectively.

The data represented that supplementation of firm concentrations of the investigated compounds to the blank solution shifted both anodic and cathodic branches of the polarization curves towards little current densities, which refer to the retardation of both anodic and cathodic reactions causing inhibition of carbon steel corrosion. Since, the inhibitor exhibited anodic and cathodic inhibition effects with a little shift in E_{corr} value to more anodic potentials, it could be deduced that such synthesized compounds perform as mixed-type inhibitors with anodic domination. The values of % IE were found to increase with increasing inhibitors concentrations and the extent of inhibition efficiencies of the compounds, at the same concentrations, followed the order: **LM > LM–Co > LN > LN–Co**, in consistent with the outcome acquired from WL measurements.

3.5.3 Electrochemical Impedance Spectroscopy (EIS) Measurements

Corrosion of carbon steel in 1.0 M HCl solution was also examined by EIS measurements. Nyquist plots of carbon steel corrosion in 1.0 M HCl solution containing various concentrations of the synthesized compounds are plotted but only Nyquist plots for the complex **LM–Co** is plotted in Fig. 6. The values of charge transfer resistance (R_{ct}) and %

Table 5 Polarization data for the corrosion of carbon steel in 1.0 M HCl solution, without and with of several concentrations of the synthesized compounds at 25 °C

Inh.	Concn. (ppm)	$-E_{corr}$ (mV(SCE)	β_a (mV/dec.)	$-\beta_c$ (mV/dec.)	i_{corr} (μA/cm^2)	% IE	θ
	0	**448**	**96**	**74**	**610**	–	–
LM	100	444	107	96	189	69	0.69
	200	438	114	98	134	78	0.78
	300	439	103	102	92	85	0.85
	400	431	118	97	49	92	0.92
	500	425	115	107	37	94	0.94
LN	100	440	105	113	231	62	0.62
	200	434	108	111	159	74	0.74
	300	434	111	115	104	83	0.83
	400	432	107	119	73	88	0.88
	500	430	115	123	52	91	0.91
LM–Co	100	442	99	111	214	65	0.65
	200	441	110	104	146	76	0.76
	300	434	115	98	104	83	0.83
	400	421	124	114	67	89	0.89
	500	417	131	118	49	92	0.92
LN–Co	100	446	109	93	244	60	0.60
	200	437	101	98	165	73	0.73
	300	431	114	104	122	80	0.80
	400	443	124	96	104	83	0.83
	500	424	119	112	85	86	0.86

Bold font is given to discriminate the compounds codes

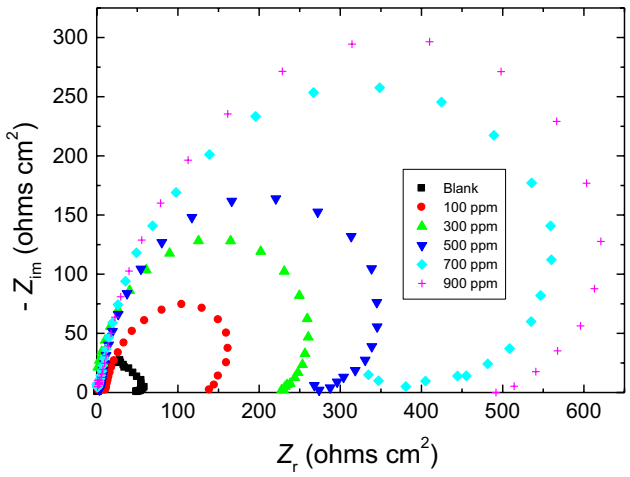

Fig. 6 Nyquist plots for the corrosion of carbon steel in 1.0 M HCl solution in the absence and presence of different concentrations of the complex **LM–Co** at 25 °C

IE (Table 6) were also computed from R_{ct} from the following equation [41]:

$$\%\,\mathrm{IE} = \left[1 - \frac{R_{ct}}{R_{ct(inh)}}\right] \times 100 \tag{4}$$

where R_{ct} and $R_{ct(inh)}$ are the charge transfer resistance values in the absence and presence of inhibitor, respectively.

Table 6 Values of R_{ct}, % IE and **θ** of several concentrations of the synthesized compounds for the corrosion of carbon steel in 1.0 M HCl solution at 25 °C

Inh.	Concn. (ppm)	R_{ct}	% IE	θ
	0	**55**	–	–
LM	100	157	65	0.65
	200	275	80	0.80
	300	123	87	0.87
	400	560	90	0.90
	500	690	92	0.92
LN	100	141	61	0.61
	200	204	73	0.73
	300	290	81	0.81
	400	393	86	0.86
	500	460	88	0.88
LM–Co	100	162	66	0.66
	200	261	79	0.79
	300	340	86	0.86
	400	560	90	0.90
	500	613	91	0.91
LN–Co	100	150	63	0.63
	200	205	73	0.73
	300	275	80	0.80
	400	344	84	0.84
	500	365	85	0.85

Bold font is given to discriminate the compounds codes

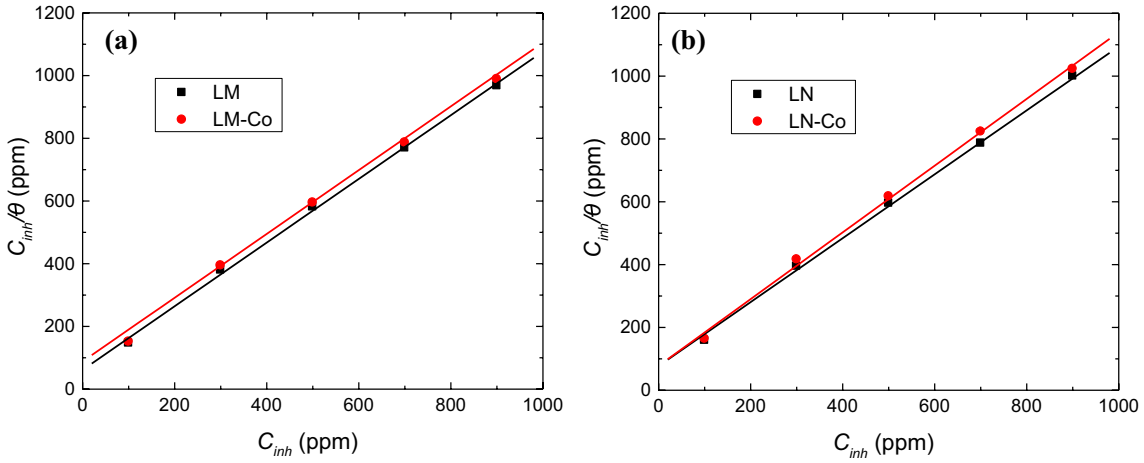

Fig. 7 Langmuir adsorption isotherms for the synthesized ligands and their complexes: **a LM** and **b LN**, adsorbed the on carbon steel surface in 1.0 M HCl solution at 25 °C

Figure 6 illustrated that, for all examined compounds, the size of the capacitive semicircle of carbon steel in 1.0 M HCl solution were found to increase significantly after the addition of the inhibitor approving that corrosion resistance of carbon steel occurs in the presence of the examined compounds, and this behavior increased with increasing inhibitor concentration.

3.5.4 Adsorption Isotherm

Adsorption of the synthesized organic compounds (inhibitors, inh.) in aqueous solution involves substitution of adsorbed water molecules ($H_2O_{(ads)}$) by organic compounds according to the following equation [42]:

$$\mathrm{Inh.}_{(sol)} + \mathrm{nH_2O}_{(ads)} \rightarrow \mathrm{Inh.}_{(ads)} + \mathrm{nH_2O}_{(sol)}. \quad (5)$$

The interaction between organic compounds and carbon steel surface could be extracted from the so-called adsorption isotherms which feed useful insights into the corrosion inhibition mechanism. Fitting of the experimental data to various isotherms including Langmuir, Freundlich, Temkin and Flory–Huggins isotherms has been examined. The experimental results in the existing study revealed that the adsorption of the synthesized compounds on the examined steel surface in 1.0 M HCl solution was found to in a good accord with Langmuir adsorption isotherm, illustrated in Fig. 7, which is given by the following equation [43]:

$$\frac{C_{inh}}{\theta} = \frac{1}{K_{ads}} + C_{inh} \quad (6)$$

where K_{ads} is the adsorptive equilibrium constant.

4 Conclusions

Two new ligands based on 1,3,4-thiadiazolethiosemicarbazone, which synthesized by the condensation reaction of 2,3-disubstituted-5-acetyl-1,3,4-thiadiazole derivatives with thiosemicarbazide in acidic medium, have been used for the synthesis of Co(II) complexes. The structures and purity of both ligands and their complexes have been identified applying various analytical and spectral tools. Analytical data indicated that the complexes have been formed in the molar ratio 1:1 (L:M) having the formulae [(**LM**)Co(OAc)$(H_2O)_2$]H_2O (**LM–Co**) and [(**LN**)Co(OAc)$(H_2O)_2$]0.5CH_3OH (**LN–Co**); where **LM** and **LN** are 1,3,4-thiadiazolethiosemicarbazone ligands with methyl and nitro substituents, respectively. Careful comparing of the results of IR-spectra of the two ligand derivatives with those for their metal chelates clarified that ligands acted as monobasic tridentate connecting to the metal ion center through nitrogen atoms of azomethine group and thiadiazole ring and deprotonated SH group. UV–Vis spectra and magnetic moment data showed that both complexes have octahedral arrangements. The synthesized compounds were utilized as efficient inhibitors for the corrosion of carbon steel in 1.0 M HCl solution. Adsorption of the tested compounds on carbon steel follows the Langmuir isotherm. The extent of inhibition efficiencies of the compounds followed the order: **LM > LM–Co > LN > LN–Co**. The results obtained from the applied techniques are compatible with each other.

References

1. D. Karcz, A. Matwijczuk, B. Boron, B. Creaven, L. Fiedor, A. Niewiadomy, M. Gagos, Isolation and spectroscopic

characterization of Zn(II), Cu(II), and Pd(II) complexes of 1,3,4-thiadiazole-derived ligand. J. Mol. Struct. **1128**, 44–50 (2017)
2. L.M.T. Frija, A.J.L. Pombeiro, M.N. Kopylovich, Coordination chemistry of thiazoles, isothiazoles and thiadiazoles. Coord. Chem. Rev. **308**, 32–55 (2016)
3. K. Zhang, H. Zheng, C. Hua, M. Xin, J. Gao, Y. Li, Novel fluorescent N,O-chelated fluorine-boron benzamide complexes containing thiadiazoles: synthesis and fluorescence characteristics. Tetrahedron **74**, 4161–4167 (2018)
4. C. Richardson, P.J. Steel, D.M. D'Alessandro, P.C. Junk, F.R. Keene, Mono- and di-nuclear complexes of the ligands 3,4-di(2-pyridyl)-1,2,5-oxadiazole and 3,4-di(2-pyridyl)-1,2,5-thiadiazole; new bridges allowing unusually strong metal–metal interactions. J. Chem. Soc. Dalton Trans. (2002). https://doi.org/10.1039/B202954E
5. G.-L. Wen, Y.-Y. Wang, P. Liu, C.-Y. Guo, W.-H. Zhang, Q.-Z. Shi, A series of 1-D to 3-D metal–organic coordination architectures assembled with V-shaped bis(pyridyl)thiadiazole under co-ligand intervention. Inorg. Chim. Acta **362**, 1730–1738 (2009)
6. B. Ardan, Y. Slyvka, E. Goreshnik, M. Myskiv, First N-allylaminothiadiazole copper(i) π-complexes: synthesis and structural peculiarities of $Cu(L)CF_3SO_3]$ and $[Cu_2(L)_2(H_2O)_2](SiF_6) \cdot 2.5H_2O$ compounds (L = 2-(allyl)-amino-5-methyl-1,3,4-thiadiazole). Acta Chim. Slov. **60**, 484–490 (2013)
7. S. Chandra, S. Gautam, A. Kumar, M. Madan, Coordination mode of pentadentate ligand derivative of 5-amino-1,3,4-thiadiazole-2-thiol with nickel(II) and copper(II) metal ions: synthesis, spectroscopic characterization, molecular modeling and fungicidal study. Spectrochim. Acta A **136**, 672–681 (2015)
8. A. Smaili, L.A. Rifai, S. Esserti, T. Koussa, F. Bentiss, S. Guesmi, A. Laachir, M. Faize, Copper complexes of the 1,3,4-thiadiazole derivatives modulate antioxidant defense responses and resistance in tomato plants against fungal and bacterial diseases. Pestic. Biochem. Physiol. **143**, 26–32 (2017)
9. H. Zine, L.A. Rifai, T. Koussa, F. Bentiss, S. Guesmi, A. Laachir, K. Makroum, M. Belfaiza, M. Faize, The mononuclear nickel (II) complex bis(azido-kN)bis[2,5-bis(pyridin-2-yl)-1,3,4-thiadiazole-κ2N2, N3]nickel(II) protects tomato from Verticillium dahliae by inhibiting the fungal growth and activating plant defenses. Pest Manag. Sci. **73**, 188–197 (2017)
10. M. El Azhar, B. Mernari, M. Traisnel, F. Bentiss, M. Lagrenée, Corrosion inhibition of mild steel by the new class of inhibitors [2,5-bis(n-pyridyl)-1,3,4-thiadiazoles] in acidic media. Corrosion sci. **43**, 2229–2238 (2001)
11. F. Bentiss, M. Lebrini, H. Vezin, M. Lagrené, Experimental and theoretical study of 3-pyridyl-substituted 1,2,4-thiadiazole and 1,3,4-thiadiazole as corrosion inhibitors of mild steel in acidic media. Mater. Chem. Phys. **87**, 18–23 (2004)
12. F. Bentiss, M. Traisnel, M. Lagrenee, Influence of 2,5-bis(4-dimethylaminophenyl)-1,3,4-thiadiazole on corrosion inhibition of mild steel in acidic media. J. Appl. Electrochem. **31**, 41–48 (2001)
13. M.A. Arenos, M. Bethencourt, F.G. Botana, J. Domborenena, M. Marcos, Inhibition of 5083 aluminium alloy and galvanised steel by lanthanide salts. Corros. Sci. **43**, 157–170 (2001)
14. D. Gustincic, A. Kokalj, DFT study of azole corrosion inhibitors on Cu_2O model of oxidized copper surfaces: I. Molecule–surface and Cl–surface bonding. Metals **8**, 311–338 (2018)
15. I.A. Arkhipushkin, K.S. Shikhaliev, A.Y. Potapov, L.V. Sapronova, L.P. Kazansky, Inhibition of brass (80/20) by 5-mercaptopentyl-3-amino-1,2,4-triazole in neutral solutions. Metals **7**, 488–500 (2017)
16. A. Fawzy, M. Abdallah, I.A. Zaafarany, S.A. Ahmed, I.I. Althagafi, Thermodynamic, kinetic and mechanistic approach to the corrosion inhibition of carbon steel by new synthesized amino acids-based surfactants as green inhibitors in neutral and alkaline aqueous media. J. Mol. Liq. **265**, 276–291 (2018)
17. A. Fawzy, I.A. Zaafarany, H.M. Ali, M. Abdallah, Corrosion inhibition performance of a novel cationic surfactant for protection of carbon steel pipeline in acidic media. Int. J. Electrochem. Sci. **13**, 4575–6842 (2018)
18. R.F. Godec, M.G. Pavlovic, Synergistic effect between non-ionic surfactant and halide ions in the forms of inorganic or organic salts for the corrosion inhibition of stainless-steel X4Cr13 in sulphuric acid. Corros. Sci. **58**, 192–201 (2012)
19. E. Khamis, M.A. Ameer, N.M. AlAndis, G. Al-Senani, Effect of thiosemicarbazones on corrosion of steel in phosphoric acid produced by wet process. Corrosion **56**, 127–138 (2000)
20. N. Karakus, K. Sayin, The investigation of corrosion inhibition efficiency on some benzaldehyde thiosemicarbazones and their thiole tautomers: computational study. J. Taiwan Inst. Chem. E. **48**, 95–102 (2015)
21. C. Verma, L.O. Olasunkanmi, E.E. Ebenso, M.A. Quraishi, Substituents effect on corrosion inhibition performance of organic compounds in aggressive ionic solutions: a review. J. Mol. Liq. **251**, 100–118 (2018)
22. M. Yadav, S. Kumar, I. Bahadur, D. Ramjugernath, Electrochemical and quantum chemical studies on synthesized phenylazopyrimidone dyes as corrosion inhibitors for mild steel in a 15% HCl solution. Int. J. Electrochem. Sci. **9**, 3928–3950 (2014)
23. M.A. Hegazy, H.M. Ahmed, A.S. El-Tabei, Investigation of the inhibitive effect of p-substituted 4-(N,N,N-dimethyldodecylammonium bromide)benzylidene-benzene-2-yl-amine on corrosion of carbon steel pipelines in acidic medium. Corros. Sci. **53**, 671–678 (2011)
24. S.K. Saha, A. Dutta, P. Ghosh, D. Sukul, P. Banerjee, Novel Schiff-base molecules as efficient corrosion inhibitors for mild steel surface in 1 M HCl medium: experimental and theoretical approach. Phys. Chem. Chem. Phys. **18**, 17898–17911 (2016)
25. N.F. Eweiss, A.O. Osman, Synthesis of heterocycles. Part II. New routes to acetylthiadiazolines and alkylazothiazoles. J. Heterocycl. Chem. **17**, 1713–1717 (1980)
26. W.J. Geary, The use of conductivity measurements in organic solvents for the characterisation of coordination compounds. Coord. Chem. Rev. **7**, 81–122 (1971)
27. H. El-Ghamry, N. El-Wakiel, A. Khamis, Synthesis, structure, antiproliferative activity and molecular docking of divalent and trivalent metal complexes of 4H-3,5-diamino-1,2,4-triazole and α-hydroxynaphthaldehyde Schiff base ligand. Appl. Organomet. Chem. **32**, e4583 (2018)
28. M.M. Alsharekh, I.I. Althagafi, M.R. Shaaban, T.A. Farghaly, Microwave-assisted and thermal synthesis of nanosized thiazolylphenothiazine derivatives and their biological activities. Res. Chem. Intermed. **45**, 127–154 (2019)
29. H.A. El-Ghamry, M. Gaber, T.A. Farghaly, Synthesis, structural characterization, molecular modeling and DNA binding ability of Co^{II}, Ni^{II}, Cu^{II}, Zn^{II}, Pd^{II} and Cd^{II} complexes of benzocycloheptenone thiosemicarbazone ligand. Mini. Rev. Med. Chem. **19**, 1068–1079 (2019)
30. H.A. El-Ghamry, K. Sakai, S. Masaoka, K. El-Baradie, R. Issa, Synthesis and characterization of self-assembled coordination polymers of N-diaminomethylene-4-(3-formyl-4-hydroxyphenylazo)-benzenesulfonamide. J. Coord. Chem. **65**, 780–794 (2012)
31. P.F. Rapheal, E. Manoj, M.R. PrathapachandraKurup, Copper(II) complexes of N(4)-substituted thiosemicarbazones derived from pyridine-2-carbaldehyde: crystal structure of a binuclear complex. Polyhedron **26**, 818–828 (2007)
32. K. Nakamoto (ed.), *Infrared spectra of inorganic and coordination compounds* (Wiley, New York, 1986)

33. D.-D. Yang, R. Wang, J.-L. Zhu, Q.-Y. Cao, J. Qin, H.-L. Zhu, Synthesis, crystal structures, molecular docking, in vitro monoamine oxidase-B inhibitory activity of transition metal complexes with 2-{4-[bis (4-fluorophenyl)methyl]piperazin-1-yl} acetic acid. J. Mol. Struct. **1128**, 493–498 (2017)
34. A.M. Gouda, H.A. El-Ghamry, T.M. Bawazeer, T.A. Farghaly, A.N. Abdalla, A. Aslam, Antitumor activity of pyrrolizines and their Cu(II) complexes: design, synthesis and cytotoxic screening with potential apoptosis-inducing activity. Eur. J. Med. Chem. **145**, 350–359 (2018)
35. M. Shakir, A. Abbasi, M. Azam, A.U. Khan, Synthesis, spectroscopic studies and crystal structure of the Schiff base ligand L derived from condensation of 2-thiophenecarboxaldehyde and 3,3′-diaminobenzidine and its complexes with Co(II), Ni(II), Cu(II), Cd(II) and Hg(II): comparative DNA binding studies of L and its Co(II), Ni(II) and Cu(II) complexes. Spectrochim. Acta A **79**, 1866–1875 (2011)
36. N.H. Yarkandi, H.A. El-Ghamry, M. Gaber, Synthesis, spectroscopic and DNA binding ability of CoII, NiII, CuII and ZnII complexes of Schiff base ligand (E)-1-(((1H-benzo[d]imidazol-2-yl)methylimino)methyl)naphthalen-2-ol. X-ray crystal structure determination of cobalt (II) complex. Mater. Sci. Eng., C **75**, 1059–1067 (2017)
37. A.B.P. Lever, *Inorganic electronic spectroscopy*, 2nd edn. (Elsevier, Amsterdam, 1984)
38. M. Pfaller, L. Burmeister, M.A. Bartlett, M.G. Rinaldi, Multicenter evaluation of four methods of yeast inoculum preparation. J. Clin. Microbiol. **26**, 1437–1441 (1988)
39. L.B. Tang, G.N. Mu, G.H. Liu, The effect of neutral red on the corrosion inhibition of cold rolled steel in 1.0 M hydrochloric acid. Corros. Sci. **45**, 2251–2262 (2003)
40. P. Manjula, S. Manonmani, P. Jayaram, S. Rajendran, Corrosion behaviour of carbon steel in the presence of N-cetyl-N,N,N-trimethylammonium bromide, Zn^{2+} and calcium gluconate. Anti-Corros. Methods Mater. **48**, 319–324 (2001)
41. H. Ma, S. Chen, L. Niu, S. Zhao, S. Li, D. Li, Inhibition of copper corrosion by several Schiff bases in aerated halide solutions. J. Appl. Electrochem. **32**, 65–72 (2002)
42. M. Abdallah, H.M. Altass, B.A. Al Jahdaly, M.M. Salem, Some natural aqueous extracts of plants as green inhibitor for dissolution of carbon steel in 0.5 M sulfuric acid. Green Chem. Lett. Rev. **11**, 189–196 (2018)
43. M. Christov, A. Popova, Adsorption characteristics of corrosion inhibitors from corrosion rate measurements. Corros. Sci. **46**, 1613–1620 (2004)